THE ASTROPHYSICAL JOURNAL, 320:319–332, 1987 September 1

THE SPECTRAL EVOLUTION OF DWARF NOVA OUTBURSTS

JOHN K. CANNIZZO AND SCOTT J. KENYON
Harvard-Smithsonian Center for Astrophysics
Received 1986 November 21; accepted 1987 February 26

ABSTRACT

We present calculations of the spectral evolution of disk instability models for dwarf nova outbursts. Observed stellar spectra are used to model the radiation emitted by optically thick annuli within the disk. Our general findings are in accord with those of Smak (1984*b*) and Pringle, Verbunt, and Wade (1986).

Eruptions in disks with low background accretion rates begin near the white dwarf, and the continuum flux rises simultaneously at all wavelengths. These "inside-out" outbursts have round light curves at 1350 Å and present two minima in the evolution of the $m_{4500} - m_{5550}$ color index as a function of time. Outbursts in disks with higher mass-accretion rates commence near the outer edge of the disk. The optical flux rises before the UV flux by $\Delta t \sim 0.1$–0.25 day for the parameters chosen in this study; this UV delay is smaller than the $\Delta t \lesssim 1$ day inferred for disks which emit as blackbodies. We discuss effects which can influence the UV delay and conclude that larger UV delays seem possible for disks computed with different physical assumptions.

Comparisons of theories for dwarf nova eruptions with observations currently require multifrequency spectroscopic data, which are difficult to obtain with available instruments. We propose that the "dwarf nova oscillations" might be another source of information concerning the evolution of the inner disk and that detailed observations of this phenomenon could be used to test the various outburst mechanisms.

Subject headings: stars: accretion — stars: binaries — stars: dwarf novae — stars: evolution

I. INTRODUCTION

Cataclysmic variables (CVs) are evolved binary systems consisting of a white dwarf primary and a Roche-lobe filling secondary of spectral type K or M. The red dwarf loses material through the inner Lagrangian point; this matter forms a disk and eventually accretes onto the white dwarf. Viscous stresses which couple to the orbital shear are responsible for the accretion process. The physical origin of these stresses remains a mystery, so observations of the time-dependent behavior of disks are necessary to place limits on the magnitude of the viscosity.

Dwarf novae comprise a subclass of CVs distinguished by roughly periodic outbursts which last for days to weeks and recur on time scales of weeks to years. These eruptions are currently thought to result from an instability in the envelope of the secondary star (Bath 1985 and references therein) or in the accretion disk itself (Smak 1984*a* and references therein). With the wealth of multifrequency data obtained for dwarf novae in the past few years (Szkody 1981, 1982, 1985; Wu and Panek 1982, 1983; Wade 1982; Klare *et al.* 1982; Hassall *et al.* 1983; Hassall, Pringle, and Verbunt 1985; Hassall 1985; Polidan and Holberg 1984; Verbunt *et al.* 1984; la Dous *et al.* 1985; Schwarzenberg-Czerny *et al.* 1985), it is now possible to compare theory and observations for these systems in detail. In this paper, we continue investigations of the disk instability model by computing the spectral development of the accretion disk through a complete limit cycle. The physical model for our calculations is presented in § II, while the computations themselves are described in § III. A comparison of our results with observations is discussed in § IV, and we conclude with a brief summary in § V.

II. ACCRETION DISK MODEL

a) Review of the Limit Cycle Mechanism

Various studies have detailed the physics of the disk instability model (Osaki 1974; Hoshi 1979; Meyer and Meyer-Hofmeister 1981, 1982, hereafter MM81, MM82; Smak 1982; Cannizzo, Ghosh, and Wheeler 1982, hereafter CGW; Faulkner, Lin, and Papaloizou 1983, hereafter FLP; Papaloizou, Faulkner, and Lin 1983, hereafter PFL; Lin, Papaloizou, and Faulkner 1985, hereafter LPF; Meyer and Meyer-Hofmeister 1984, hereafter MM84; Smak 1984*b*; Mineshige and Osaki 1983, 1985, hereafter MO83 and MO85; Cannizzo and Wheeler 1984, hereafter CW; Cannizzo, Wheeler, and Polidan 1986, hereafter CWP; Cannizzo, Shafter, and Wheeler 1987). Numerical solutions of the vertical structure of the classical Shakura and Sunyaev (1973) "α-disk" have revealed an "S-shaped" relationship between the integrated viscosity and surface density when the disk midplane temperature lies near 10^4 K (Hoshi 1979; MM81, MM82; Smak 1982; CGW). Thermal instabilities occur where the surface density, Σ, exhibits a maximum and a minimum, and these instabilities bring about phase transitions between the two allowed states of temperature and viscosity. The disk resides in the cold state during quiescence and stores matter lost by the secondary. Hence the surface density approaches the critical surface density, $\Sigma_{\rm max}$. The annulus that first reaches $\Sigma_{\rm max}$ begins runaway heating to the hot phase. Thin rings of enhanced surface density traveling to larger and smaller radii communicate the onset of this phase transition to most of the disk. The eruption begins near the inner disk edge if the secondary mass transfer rate, $\dot{M}_T$, is small, and near the outer edge if $\dot{M}_T$ is

large (Smak 1984*b*; MO83; MM84; CWP; Pringle, Verbunt, and Wade 1986, hereafter PVW). This behavior leads to differences in the light curves produced by the bursts which are directly observable (Smak 1984*b*; CWP; Cannizzo and Kenyon 1985; PVW). When the transition to the high state is complete, material is redistributed into the classical "outer" disk of Shakura and Sunyaev (1973). A cooling transition eventually transforms the disk back to the cool phase as material accretes onto the central white dwarf. This transition begins at large radii and moves inward; since the time scale for the transition wave to traverse the disk is short compared to the accretion (i.e., viscous) time scale, only a fraction of the stored matter is accreted ($\sim 1\%$ to 10%).

b) Steady-State Physics

The vertical structure of the thin, steady-state accretion disks expected in CV systems has been thoroughly described by MM82, FLP, and CW. Three parameters derived from the vertical integrations comprising the extensive parameter study presented in CW are of interest for the time-dependent evolution considered in this paper: the integrated viscosity $\nu\Sigma = \int \nu(z)\rho(z)dz$, and the critical surface densities $\Sigma_{\rm min}$ and $\Sigma_{\rm max}$. We require scaling laws which depend on the surface density Σ, radius R, and viscosity parameter α (the critical Σ's depend on radius and α), and parametrize the viscosity through the effective temperature, T_e, where $\sigma T_e^4 = (9/8)\Omega^2\nu\Sigma$. We divide the "S-shaped curve" (displayed in Fig. 11 of CW) into the five straight line segments depicted schematically in Figure 1 and employ a power-law fit to $T_e(\Sigma, R, \alpha)$ within each region. The vertical structure of solutions lying on the cold branch is complicated by convection, varying forms of the opacity, and the onset of optically thin conditions, so it is necessary to divide the cold state into four different regimes. The hot branch is physically much simpler, and the effective temperature can be represented by a single fit. The scaling laws for T_e are given by

$$T_e(1) = 10^{3.62}\ \mathrm{K}\ \Sigma_{2.5}^{0.36}\alpha_{-2}^{0.29}R_{10.5}^{-0.48} \quad (1)$$

$$T_e(2) = 10^{2.96}\ \mathrm{K}\ \Sigma_{2.5}^{0.95}\alpha_{-2}^{0.82}R_{10.5}^{-1.1} \quad (2)$$

$$T_e(3) = 10^{2.42}\ \mathrm{K}\ \Sigma_{2.5}^{2.2}\alpha_{-2}^{1.41}R_{10.5}^{2.41}\ , \quad \Sigma_{2.5} < 10^{0.49}\alpha_{-2}^{0.59}R_{10.5}^{1.05} \quad (3)$$

$$T_e(4) = 10^{3.25}\ \mathrm{K}\ \Sigma_{2.5}^{0.20}\alpha_{-2}^{0.24}R_{10.5}^{-0.31}\ , \quad \Sigma_{2.5} < 10^{0.39}\alpha_{-2}^{-0.52}R_{10.5}^{1.05} \quad (4)$$

$$T_e(5) = 10^{3.1}\ \mathrm{K}\ \alpha_{-2}^{0.2}R_{10.5}^{-0.1}\ , \quad \Sigma_{2.5} < 10^{-0.6}\alpha_{-2}^{-0.4}R_{10.5}^{1.05}\ , \quad (5)$$

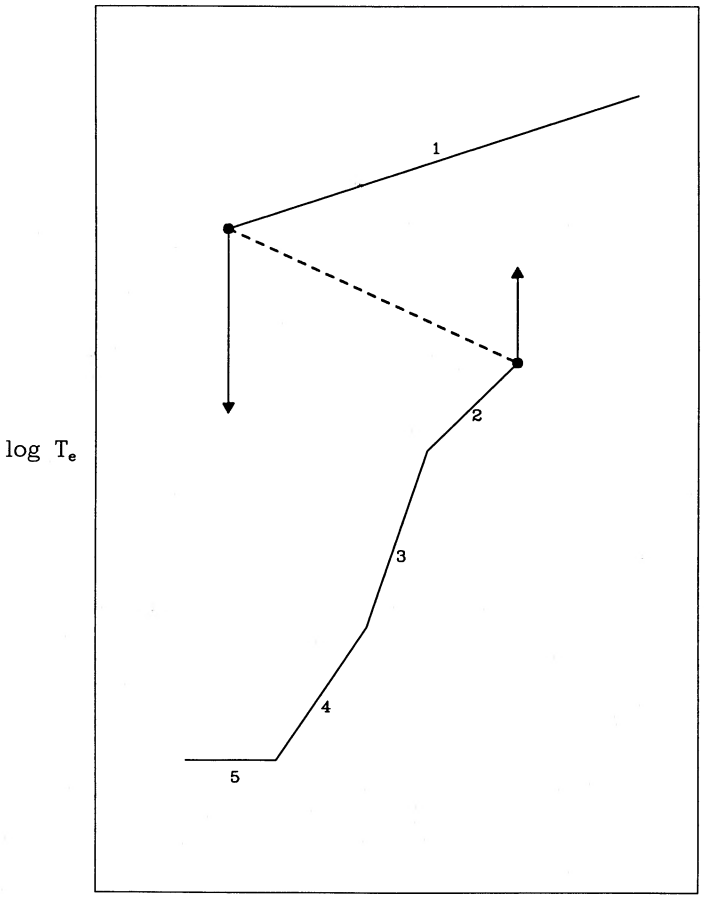

FIG. 1.—Schematic representation of the $T_e - \Sigma$ relation used to parametrize the viscosity. The hot phase is confined to region 1, while the cold phase consists of regions 2–5. The critical values of the surface density at which phase transitions begin are indicated by the filled circles. Note that the $T_e - \Sigma$ relation indicated by the dashed line is not accessible to evolving disks.

where Σ and R are expressed in cgs units. The notation x_y indicates $x/10^y$. The hot phase is characterized by equation (1), while equations (2)–(5) describe the cold phase. The critical values of the surface density are

$$\Sigma_{\max} = 10^{3.3}\ \mathrm{g\ cm^{-2}}\ \alpha_{-2}^{-0.86} R_{10.5}^{1.05} \quad (6)$$

$$\Sigma_{\min} = 10^{3.04}\ \mathrm{g\ cm^{-2}}\ \alpha_{-2}^{-0.86} R_{10.5}^{1.05}\ . \quad (7)$$

Note that the dashed line segment in Figure 1 is inaccessible to evolving disks (Bath and Pringle 1982).

Disks in cataclysmic variables have negligible self-gravity compared to that of the central white dwarf, so the mass dependence of the scaling laws for $T_e(R, \Sigma, \alpha)$ enters through the rotational frequency, $\Omega = (GM_1/R^3)^{1/2}$, where M_1 is the mass of the white dwarf. We have adopted $M_1 = 1\ M_\odot$ for equations (1) to (5); these relations scale as $f(R^{-1/3})$ for other choices of M_1.

For comparison, the scaling laws for effective temperature and critical surface densities used by PVW are (cf. MM81; FLP)

$$T_{\mathrm{hot}} = 10^{3.67}\ \mathrm{K}\ \Sigma_{2.5}^{0.38} \alpha_{-2}^{0.26} R_{10.5}^{-0.50} \quad (8)$$

$$T_{\mathrm{cold}} = 10^{3.37}\ \mathrm{K}\ \Sigma_{2.5}^{0.25} \alpha_{-2}^{0.25} R_{10.5}^{-0.38} \quad (9)$$

$$\Sigma_{\max} = 10^{3.2}\ \mathrm{g\ cm^{-2}}\ \alpha_{-2}^{-0.70} R_{10.5}^{1.10} \quad (10)$$

$$\Sigma_{\min} = 10^{2.92}\ \mathrm{g\ cm^{-2}}\ \alpha_{-2}^{-0.70} R_{10.5}^{1.15}\ , \quad (11)$$

while Smak (1984*b*) employs

$$T_{\mathrm{hot}} = 10^{3.65}\ \mathrm{K}\ \Sigma_{2.5}^{0.36} \alpha_{-2}^{0.29} R_{10.5}^{-0.47} \quad (12)$$

$$T_{\mathrm{cold}} = 10^{3.29}\ \mathrm{K}\ \Sigma_{2.5}^{0.36} \alpha_{-2}^{0.29} R_{10.5}^{-0.47} \quad (13)$$

$$\Sigma_{\max} = 10^{3.25}\ \mathrm{g\ cm^{-2}}\ \alpha_{-2}^{-0.71} R_{10.5}^{1.07} \quad (14)$$

$$\Sigma_{\min} = 10^{2.97}\ \mathrm{g\ cm^{-2}}\ \alpha_{-2}^{-0.71} R_{10.5}^{1.07}\ . \quad (15)$$

Note that the agreement between the various scaling laws is quite good.

c) *Time-Dependent Physics*

Results of previous investigations have emphasized that $\Sigma_{\max}$ must be large in comparison to $\Sigma_{\min}$ if the instability is to result in eruptions resembling those observed in dwarf novae. This can be accomplished if the viscosity in the hot phase is significantly larger than that in the cold phase (i.e., $\alpha_{\mathrm{hot}} > \alpha_{\mathrm{cold}}$; Smak 1984*b*; MO83; MO85; MM84; CWP; PVW). For simplicity, we varied α as a step function for the calculations described in this paper and set $\alpha_{\mathrm{cold}} = 0.02$ and $\alpha_{\mathrm{hot}} = 0.1$.

The viscous evolution of the accretion disk is treated using the method described by Bath and Pringle (1981). In addition to evolving the surface density, we continually inject material into the outer disk (cf. LPF) and deal with phase transitions between the two viscosity states. Whereas previous studies have employed an energy equation to compute the thermal instability, we handle the transitions in the following simplified manner. Heating begins when Σ surpasses the critical value $\Sigma_{\max}$ in any annulus, and cooling sets in when Σ drops below $\Sigma_{\min}$. These "heating" and "cooling" processes serve as the phase transitions between the two states and are executed by linearly varying T_e between $T_{e,\mathrm{cold}}$ and $T_{e,\mathrm{hot}}$ on a time scale $\beta/(\alpha\Omega)$, where β is the ratio of the specific heat, c_p, to the ideal gas constant $\mathscr{R}/\mu$ averaged over the course of the transition (Meyer 1984; PVW). As material evolves from the cold state ($T \sim 4000$ K) to the hot state ($T \sim 100{,}000$ K), it traverses the hydrogen partial ionization region at $T \sim 15{,}000$ K where c_p is large (~ 30–$100\ \mathscr{R}/\mu$). The value of c_p is nearly that of a classical monotonic gas, $5\mathscr{R}/2\mu$, during most of this transition. We adopt $\beta = \langle c_p/(\mathscr{R}/\mu)\rangle = 7$ as an average and note that the effect of varying β by a factor of ~ 2 is small (PVW).

Besides its conceptual simplicity, this prescription is less prone to numerical instabilities than its predecessor (described in CWP). More importantly, the physics of the "snowplow" and "snow shovel" effects (LPF) associated with the transition fronts is the same as in previous studies (PFL; LPF; MM84; MO83; MO85; Smak 1984*b*; CWP), and the evolution of the flux density at various wavelengths is unchanged. Indeed, we find that the scaling laws for $\Sigma_{\min}(\alpha, R)$, $\Sigma_{\max}(\alpha, R)$, and $\nu(\Sigma, \alpha, R)$ are at least as important in determining the time scales and spectral evolution as is the thermal treatment, and these scaling laws are sensitive to the treatment of convection, as well as the opacity and equation of state tables (MM81; MM82; Smak 1982; CGW; FLP; MO83; CW; Cabot *et al.* 1986; Meyer-Hofmeister 1987). Since the scaling laws developed by these groups vary by up to a factor of ~ 3 in certain circumstances, specific values for α and $\dot{M}_T$ derived for a given dwarf nova system are uncertain by a similar factor. Hence we believe that a more detailed treatment of the thermal physics is unwarranted until the α-prescription is supplanted by a physical model for the viscosity in an accretion disk.

d) *Synthetic Spectra*

The spectral evolution of the disk as a function of time is derived as follows. We assume that the disk consists of n concentric annuli, each of which has an effective temperature T_i, inner radius R_i, and outer radius R_{i+1}. If $R_{\mathrm{mid},i} = 0.5\ (R_i + R_{i+1})$ and $dR_i = R_{i+1} - R_i$, the bolometric luminosity of a given annulus is $L_{\mathrm{bol},i} = 2\pi R_{\mathrm{mid},i}\, dR_i\, \sigma T_i^4$. The total disk luminosity is the sum of $L_{\mathrm{bol},i}$ for each annulus ($L_{\mathrm{disk}} = \sum_{i=1}^{n} L_{\mathrm{bol},i}$), so the flux received at Earth is

$$F_{\mathrm{bol}} = \sum_{i=1}^{n} 2R_{\mathrm{mid},i}\, dR_i\, \sigma T_i^4 \cos i/d^2\ , \quad (16)$$

where i is the inclination of the disk to our line of sight and d is its distance. We set $i = 0°$ and $d = 10$ pc for the results described in this paper.

Equation (16) represents the total flux received from an optically thick disk; the actual flux *distribution* of a model disk is more difficult to calculate. Initial models for disks approximated the flux distribution of a given annulus by that of a perfect blackbody (Tylenda 1977; Kenyon and Webbink 1984); more rigorous attempts have calculated theoretical disk spectra using stellar atmosphere techniques for individual annuli (Schwarzenberg-Czerny and Różyczka 1977; Herter *et al.* 1979; Mayo, Wickramasinghe, and Whelan 1980; Williams 1980; Tylenda 1981; Wade 1984).

Our approach to this problem is more observationally oriented, as we employ stellar fluxes to construct a model disk spectrum. We have tabulated absolute fluxes (F_λ in ergs cm^{-2} s^{-1} Å^{-1}) covering $\lambda\lambda$1150–7400 (Wu *et al.* 1983; Jacoby, Hunter, and Christian 1984) and various broad-band color indices (Johnson 1966) for normal stars with $M_V = 0$ as functions of spectral type and luminosity class and assume that the flux distribution of a given disk annulus can be represented by one of the stars in this library. Since the gravity in a typical disk surrounding a white dwarf is $\log g \sim 3$–6, the disk spectrum is approximated as a series of main-sequence stars, with effective temperatures derived from the calibrations described

by Johnson (1966; lower main sequence) and Code *et al.* (1976; upper main sequence).

The contribution of the ith annulus to the model disk spectrum is determined from the "effective" angular diameter of a disk annulus at a distance of 10 pc,

$$\theta_i = 1.861(L_{\mathrm{bol},i}{}^*/T_i^{*4})^{1/2} , \quad (17)$$

where the starred variables are in solar units and θ_i is in milli–arc seconds. The angular diameter is related to the apparent visual magnitude, V_i, and the surface brightness parameter, $F_{V,i}$, via

$$F_{V,i} = 4.2207 - (0.1V_i + 0.5 \log \theta_i) . \quad (18)$$

The quantity $F_{V,i}$ is a function of the $V-R$ color tabulated in the stellar library (Barnes, Evans, and Moffett 1978), so the visual magnitude of an annulus may be determined from equations (17) and (18) using values for the effective temperature (spectral type) and bolometric luminosity from the hydrodynamic calculations. Once V_i is known, the tabulated fluxes of a star with effective temperature T_i are scaled by $10^{-0.4V_i}$ to derive the fluxes emitted by the annulus.

In most instances, the temperature of an annulus, T_i, is not identical to the effective temperature of a star in the library. We assume that the flux distribution of this annulus is a linear combination of library fluxes:

$$F_{\mathrm{disk}}(T_i) = f_1 F_{\mathrm{lib}}(T_1) + f_2 F_{\mathrm{lib}}(T_2) , \quad (19)$$

where $f_1 = (T_i - T_2)/(T_1 - T_2)$, $f_2 = (T_1 - T_i)/(T_1 - T_2)$, and $T_1 > T_i > T_2$. This interpolation method is not accurate at low temperatures ($T_i < 20{,}000$ K) if $T_1 - T_2$ is large. However, the stellar library is so finely spaced in T for spectral types later than B0 that equation (19) is still accurate for small T. Experiments with other weighting schemes, such as Planckian weights or weights scaled by T^4, yield results that differ by $\sim 5\%$ to 10% from those presented in this paper. The uncertainties in the input physics, including the radiative transfer, are significantly larger than 5% to 10%, so we have chosen to present results only for the weighting scheme in equation (19).

We compute the entire disk spectrum at each time step, but most of the spectral evolution of a model accretion disk can be understood by following selected narrow-band magnitudes as functions of time. We define $m_\lambda = -2.5 \log F_\lambda - 21.1$, where F_λ is the mean flux (in units of ergs cm^{-2} s^{-1} Å^{-1}) in a 20 Å bandpass centered at λ. The $m_{4500} - m_{5550}$ color presented for our models is similar to the $B-V$ color typically measured for normal stars (aside from an arbitrary normalization factor) and is not contaminated by the rapidly evolving emission or absorption features which characterize an erupting dwarf nova system. The $m_{1350} - m_{2700}$ color similarly measures the slope of the UV continuum; although it requires knowledge of the relative calibration of the short-wavelength and long-wavelength *IUE* cameras, this color avoids regions which are poorly calibrated or underexposed in the satellite ultraviolet.

The disks in our models are very cool in quiescence ($T \sim 4000$ K) and thus are very faint in the ultraviolet ($m_{1350} \sim 25$–30). We therefore assume that the quiescent flux level is set by the combination of a 20,000 K white dwarf ($R_{\mathrm{wd}} = 5 \times 10^8$ cm) and an optically thin chromosphere ($n_{\mathrm{elec}}{}^2 V = 5 \times 10^{55}$ cm^{-3}; $T_{\mathrm{elec}} = 20{,}000$ K) for the purposes of constructing model light curves. These values are representative of those found in dwarf nova systems (see, for example, Krautter, *et al.* 1981; Wu and Panek 1982; Ferguson 1983; Berriman 1984; Szkody and Mateo 1984; Shafter *et al.* 1985; Berriman, Kenyon, and Bailey 1986; Wood *et al.* 1986; Berriman, Kenyon, and Boyle 1987; and references therein), so our quiescent light levels should be close to actual values for most dwarf novae. This "model" has not been assumed for the construction of synthetic spectra; spectra presented below are calculated for the disk only.

III. RESULTS

a) Background

Previous investigations have identified two extremes in the form of the light curves produced by disk instabilities (Smak 1984*a*, *b*). Bursts which begin at a small disk radius ("inside-out") produce symmetric light curves with comparable rise and decline times, while eruptions starting at a large disk radius ("outside-in") generate asymmetric light curves with short rise times and protracted declines. A physical explanation for this difference is presented by CWP.

Smak (1984*b*) and CWP find that the optical flux leads the far-UV flux by $\sim \frac{1}{2}$ day in the asymmetric bursts, and by a lesser amount in the symmetric bursts. Although the shape of the light curves and the length of the delay are in general accord with the observations (Smak 1984*b*; CWP; Hassall *et al.* 1983; Polidan and Holberg 1984), Smak (1984*b*) and CWP used blackbodies rather than stellar fluxes to model the flux distribution of an evolving disk. Since steady-state disks constructed from stellar atmosphere models have significantly different flux distributions from those made with blackbodies (Wade 1984), it is important to verify the behavior of outside-in bursts with a different treatment of the radiative transfer. PVW used Kurucz model flux distributions to characterize accretion disk spectra and were unable to produce a significant time lag between the UV and optical flux for an outside-in burst on a small disk. One of our goals is to determine if this is a common feature of all outside-in bursts which use stellar fluxes to model the disk spectrum.

b) Computations

The model disks used to investigate the limit cycle in our calculations surround a 1 $M_\odot$ white dwarf with a radius $R_{\mathrm{wd}} = 5 \times 10^8$ cm. Material is added to the disk at an injection radius, R_{inj}, in a Gaussian configuration with a FWHM of $0.2R_{\mathrm{inj}}$ (LPF). The injection radius is assumed to be the point in the disk where the specific angular momentum equals that of matter leaving the secondary from the L_1 point (Lubow and Shu 1975). We have adopted $R_{\mathrm{inj}} = 10^{10}$ cm (small disk) and 2×10^{10} cm (large disk); these values correspond to CV systems with orbital periods, $P_{\mathrm{orb}} \sim 1$ hr and 6 hr, respectively, if the secondary star has a mass of 0.11 (P_{orb}/1 hr) $M_\odot$ (Whyte and Eggleton 1980; Shafter, Wheeler, and Cannizzo 1986, hereafter SWC). These orbital periods are comparable to those of dwarf novae having extensive multifrequency observations through a complete eruption cycle (Verbunt *et al.* 1984; Hassall, Pringle, and Verbunt 1985; PVW). Our radial grid consists of 45 points; we set the inner disk radius, $R_{\mathrm{in}} = R_{\mathrm{wd}}$, and let the outer disk radius, $R_{\mathrm{out}} = 2R_{\mathrm{inj}}$.

The critical quantity in the limit cycle calculations is the ratio, ζ, of the input mass transfer rate, $\dot{M}_T$, to the critical value above which the entire disk resides permanently in the hot state, $\dot{M}_C$ (SWC). If $\zeta \ll 1$, a system experiences inside-out eruptions; outside-in bursts occur when $\zeta \lesssim 1$. This situation arises because the time scale to enhance the surface density, Σ,

near R_{inj} is shorter than the viscous drift time only when $\dot{M}_T$ is large. The disk first reaches the critical surface density at small radii when $\dot{M}_T$ is small, because there is enough time for material to diffuse inward from R_{inj}. We find that the dividing line between the two types of eruptions lies near $\zeta \sim 0.3$. Since there is a smooth transition between inside-out and outside-in eruptions, there is a gradual change in the character of the outburst light curves as $\dot{M}_T$ is varied. The particular values of $\dot{M}_T$ used in this study were selected by qualitatively examining the visual light curves from several trial computations which had relaxed into a recurring pattern of eruptions. We take $\dot{M}_T = 10^{-10}$ and $4 \times 10^{-10}\ M_\odot\ \mathrm{yr}^{-1}$ ($\zeta = 0.10, 0.42$) for the small disk, and $\dot{M}_T = 10^{-9}$ and $4 \times 10^{-9}\ M_\odot\ \mathrm{yr}^{-1}$ ($\zeta = 0.17, 0.69$) for the large disk. Other physical parameters for the models are listed in Table 1.

c) *Evolution of Model Accretion Disks*

i) *Small Disks*

The eruption for model 1 begins at a radius of 2×10^9 cm ($\sim 4R_{wd}$) and swiftly spreads to smaller and larger radii. Initially, the rise to visual maximum is very rapid, but the evolution slows down once V reaches 7th mag (Fig. 2). The disk takes ~ 1 day to evolve from $V = 6.7$ to visual maximum at $V = 5.7$. The rise in the ultraviolet parallels the evolution in the visual, and there is no evidence for a delay between the optical and ultraviolet flux in this "inside-out" eruption. Peak

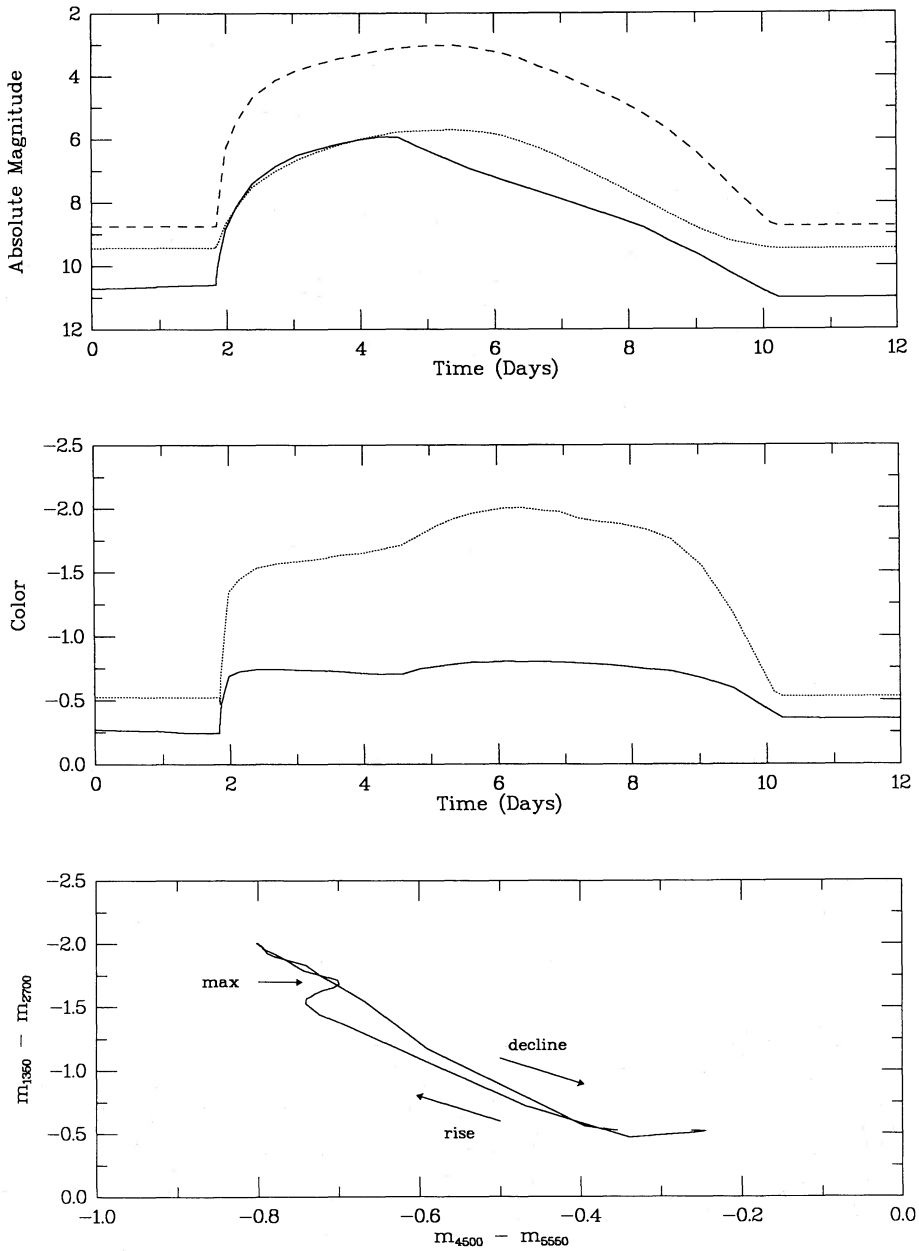

FIG. 2.—Light and color curves for an inside-out eruption in a small accretion disk (Model 1). The top panel shows the evolution of V (*solid line*), m_{1350} (*dashed line*), and m_{bol} (*dotted line*) as a function of time. The center panel presents the evolution of the optical ($m_{4500} - m_{5550}$; *solid line*) and ultraviolet ($m_{1350} - m_{2700}$; *dotted line*) colors as a function of time. The bottom panel shows the evolution of the model disk in the ultraviolet-optical color-color diagram.

TABLE 1

PHYSICAL PARAMETERS FOR MODEL ACCRETION DISKS

Model	R_{inj} (10^{10} cm)	ζ	t_{burst} (days)	t_{recur} (days)	R_{erupt}/R_{inj}
1.....	1.0	0.10	7	20	0.20
2.....	1.0	0.42	8	17	0.46
3.....	2.0	0.17	14	24	0.23
4.....	2.0	0.69	14	22	0.68

flux at 1300 Å occurs $\sim$1 day after visual maximum, and the inner disk remains hot as the outer disk cools off.

The initial rise in disk emission is accompanied by a decrease in $m_{1350} - m_{2700}$ and $m_{4500} - m_{5550}$, as shown in the middle panel of Figure 2. These colors remain nearly constant as the system evolves to visual maximum and then increase once the optical brightness begins to decline. The early optical decline is a result of material moving from the outer portions of the disk toward the central white dwarf, and the inner disk continues to increase in effective temperature (thereby becoming bluer) as V declines. This behavior continues until the rate at which material falling into the inner disk cannot compensate for the flow of material onto the white dwarf. Then the ultraviolet and optical colors increase until the system returns to its minimum state.

Synthetic disk spectra for model 1 are presented in Figure 3. Spectra on the rising branch of the light curve are plotted for

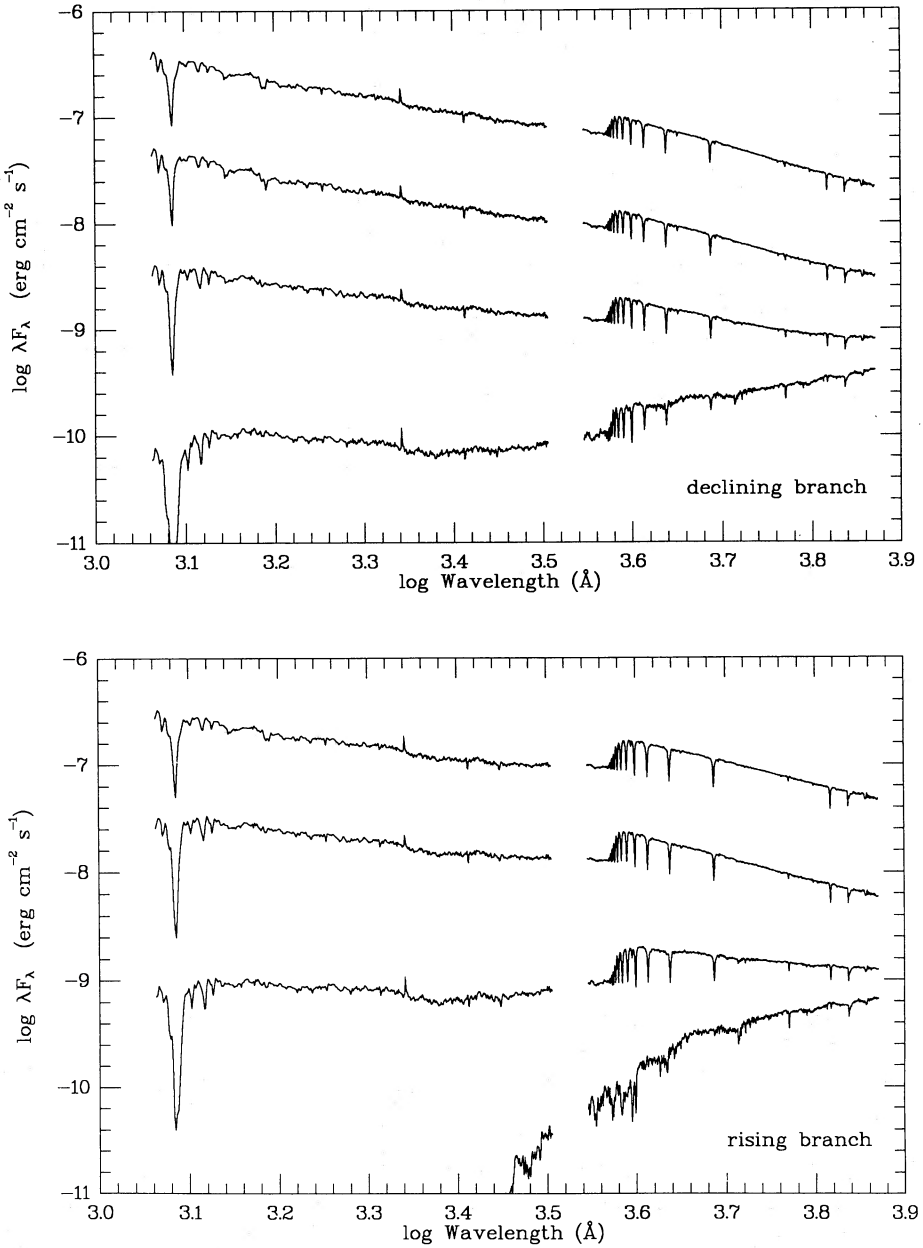

FIG. 3.—Spectral evolution for a disk undergoing an inside-out eruption (Model 1). The lower panel shows the spectral changes which occur during the rise to visual maximum; the plotted spectra correspond to $t = 0.42$, 1.87, 2.14, and 4.28 days from the bottom of the panel to the top. The upper panel presents the spectral evolution as the disk returns to quiescence at $t = 5.37$, 8.24, 9.51, and 10.11 days from top to bottom, respectively. The top spectrum in the bottom panel of this and subsequent figures corresponds to visual maximum, while the top spectrum in the top panel corresponds to ultraviolet maximum.

t = 0.42, 1.87, 2.17, and 4.28 days from the bottom to the top of the panel; spectra on the declining branch are plotted for t = 5.37, 8.24, 9.51, and 10.11 days from the top to the bottom of the panel. The quiescent disk is quite cool ($T_e \sim$ 3000 to 4000 K), and its spectrum would be dominated by radiation from the white dwarf or a disk chromosphere. As the outburst commences, the low-excitation absorption lines (Mg II and Ca II) vanish, and lines from He I, C IV, and N V strengthen. Since C IV has prominent P Cygni profiles during the eruptions of many dwarf novae (Hassall *et al.* 1983; Córdova and Mason 1982), the presence of C IV in our model spectra suggests that future analyses of P Cyg features in dwarf novae should try to account for contributions from the underlying accretion disk.

The evolution of the disk in model 2 is qualitatively similar to that of model 1, and our numerical results are summarized in Figures 4–5. The major differences between these models are (1) the rise to optical maximum is ~1 day faster for the "outside-in" eruption of model 2, and (2) the ultraviolet flux in model 2 begins to rise ~0.1 day after the optical flux. Our UV delay is somewhat smaller than that found for blackbody disks; this is a result of the flat UV flux distribution of stars with $T_e \gtrsim 10^4$ K, as noted by PVW.

The behavior of the colors in model 2 is also different from model 1. A comparison of Figures 2 and 4 shows that the colors do not have the "double-peaked" light curves characteristic of inside-out bursts, but are more rounded. The second decrease in the optical and UV colors observed in model 1 does not occur for outside-in eruptions, since an increase in mass transfer from the outer disk to the inner disk begins immediately upon transition to the hot phase. This increase in

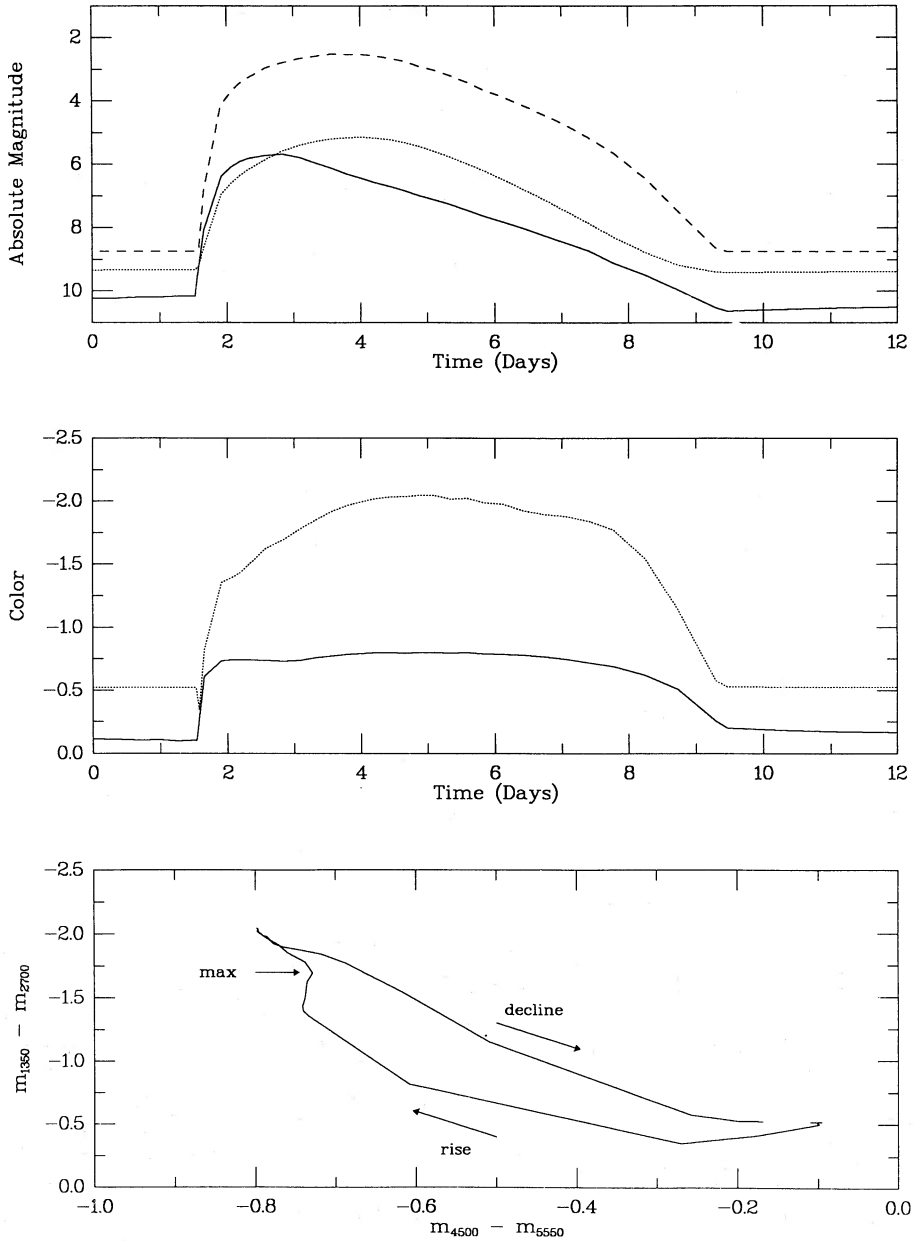

FIG. 4.—Light and color curves for an outside-in eruption in a small disk (Model 2), with panels arranged as in Fig. 2

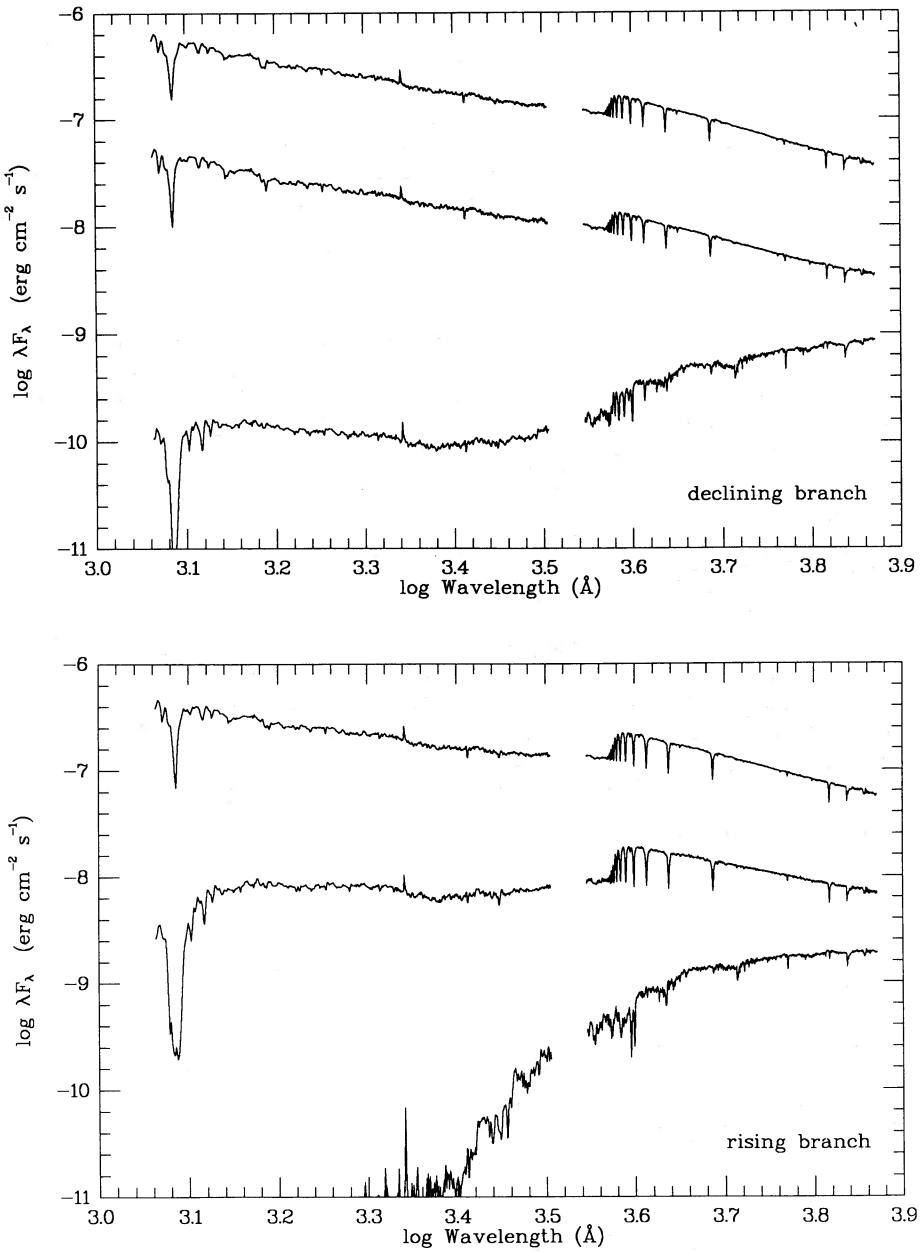

FIG. 5.—Evolution of the disk spectrum during an outside-in eruption (Model 2), with panels arranged as in Fig. 3. The lower panel plots spectra for $t = 1.54$, 1.65, and 2.83 days, while spectra at $t = 3.57$, 7.41, and 9.29 days are shown in the upper panel.

$\dot{M}$ occurs at later times in an inside-out eruption, because the outer disk must wait for the transition wave from the inner edge in model 1.

The evolution of the colors in model 2 should be qualitatively similar to that observed in eruptions initiated by an increase in mass transfer from the secondary star, because the initial luminosity increase is caused by material in the outer disk for both cases. This remark assumes that matter is introduced rapidly into the outer portions of the disk; as noted by PVW, different behavior can be induced by varying the rate at which material is introduced into the disk by the secondary star.

It is interesting that *the ultraviolet slope exceeds that of a semi-infinite, steady-state blackbody disk throughout most of the eruption of models 1 and 2.* The classical $F_\lambda \sim \lambda^{-7/3}$ law described by Lynden-Bell and Pringle (1974) corresponds to $m_{1350} - m_{2700} = -1.76$, while our models reach $m_{1350} - m_{2700} = -2$ shortly after visual maximum. Our models resemble steady-state blackbody disks only during the final rise to bolometric maximum of model 1.

Wade (1984) has noted that the spectral slope in the UV should be different from $\lambda^{-7/3}$ for disks synthesized from stellar atmospheres, because the Lyman and Balmer absorption edges redistribute flux to longer wavelengths and steepen the UV continuum over that expected from a blackbody at the same temperature. We have compared our models 1 and 2 with a sequence of steady-state disks synthesized with the stellar flux library and found that *steady-state accretion disks do not provide a good representation of the UV continuum during the declining phases of a dwarf nova outburst in a short-period*

CV system. A steady disk having the same m_{1350} as our time-dependent disks may have significantly bluer *or* redder $m_{1350} - m_{2700}$ colors (~ 0.5 mag), depending on the outburst phase (rising to maximum or declining to minimum).

To quantify this behavior, we have examined the radial dependence of the effective temperature near bolometric maximum for each of our models. We find that $d \log T/d \log R$ for the disk undergoing inside-out bursts decreases from $d \log T/d \log R = -0.5$ at the inner edge of the disk to $d \log T/d \log R = -1.25$ at the outer edge of the disk at bolometric maximum. The temperature gradient is close to the steady-state prediction of $d \log T/d \log R = -0.75$ only for a small range of radii in the middle of the disk. The relatively flat temperature gradient in the inner disk, coupled with the steep temperature gradient in the remaining disk annuli, result in disks which are much bluer in color than steady-state disks with the same bolometric luminosity. Mass transfer rates deduced from a comparison of observed and steady-state UV continuum slopes for most dwarf novae are therefore unreliable; steady-state models used in these techniques should be replaced by time-dependent models.

ii) *Large Disks*

The inside-out eruption calculated in model 3 begins at a radius of 4.6×10^9 cm ($\sim 9R_{wd}$), and resembles the model 1 outburst (Figs. 6–7). This disk is ~ 1.2 mag brighter at 1350 Å and 5550 Å at maximum than a similar eruption on a smaller disk, which is a result of a factor of 4 increase in surface area. The shapes of the light curves in the top panel of Figure 6 are remarkably similar to those in Figure 2, although the larger

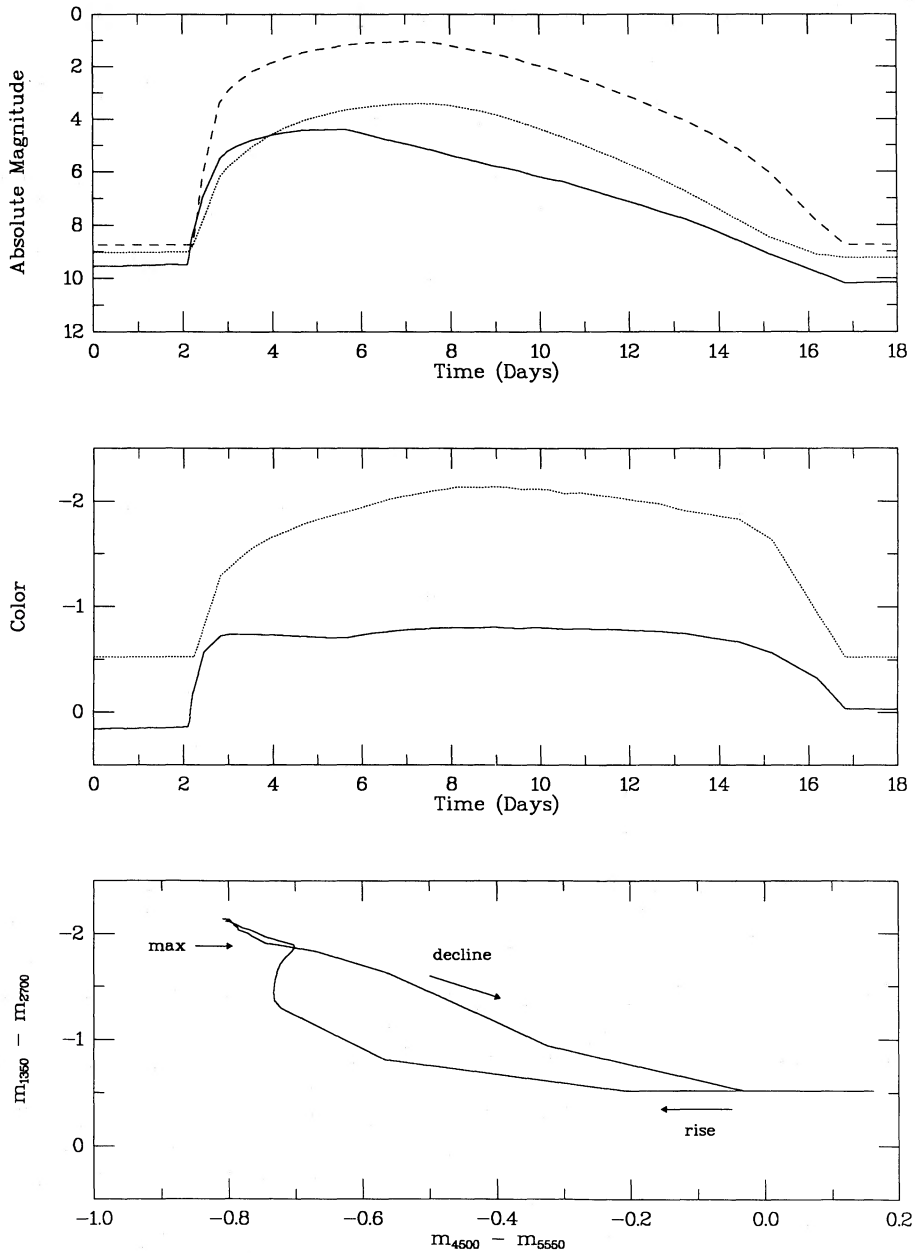

FIG. 6.—Light and color curves for an inside-out eruption in a large disk (Model 3), with panels arranged as in Fig. 2

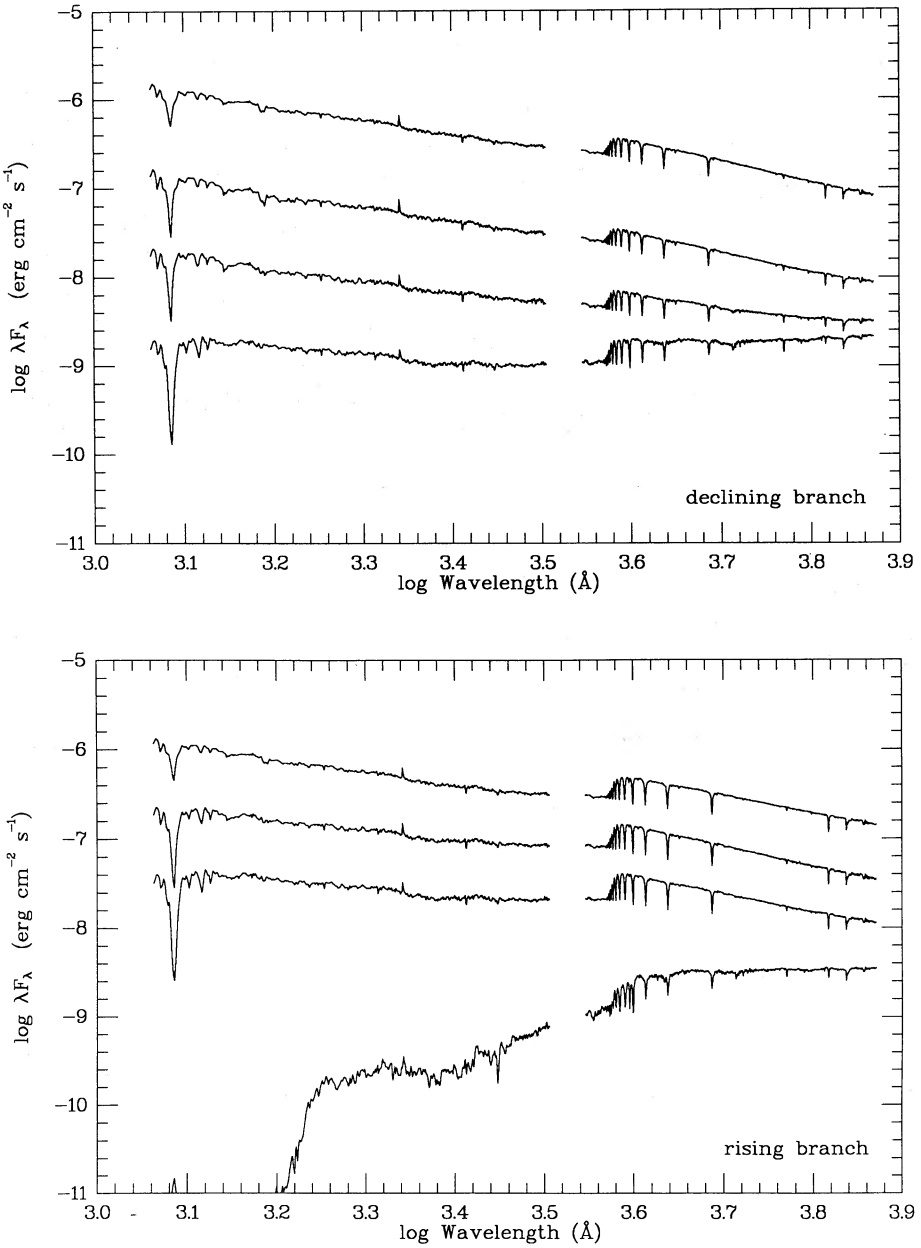

FIG. 7.—Evolution of the disk spectrum during an inside-out eruption (Model 3), with panels arranged as in Fig. 3. The lower panel plots spectra for $t = 1.79$, 1.94, 2.49, and 5.59 days, while spectra at $t = 6.97$, 10.97, 12.61, and 13.63 days are shown in the upper panel.

disk takes ~ 2 extra days to reach visual maximum. The return to minimum is also slower in this model, with the entire eruption lasting ~ 14 days (as opposed to ~ 8 days for the small disk in model 1).

The evolution of model 4 is very different from the other eruptions in this study, as shown in Figures 8–9. Unlike its smaller counterpart, the outside-in eruption of a relatively large accretion disk shows a significant delay between the rise of the optical flux and the ultraviolet flux. This is shown most clearly in the middle panel of Figure 8, which presents the evolution of the $m_{1350} - m_{2700}$ and $m_{4500} - m_{5550}$ colors as a function of time. The decrease in the optical color index from ~ 0 to ~ -0.7 is accompanied by an *increase* in the UV color index from ~ -0.5 to ~ 1. Once the optical flux has risen to within ~ 1.5 mag of maximum, the far-UV flux begins to rise and $m_{1350} - m_{2700}$ decreases from ~ 1 to -1.2. It takes ~ 0.25 day for the far-UV to respond to the transition front; after this time, the optical and ultraviolet rise together. The peak in m_{1350} occurs ~ 3 days after visual maximum, when m_{5550} has already declined by ~ 1 mag.

The spectral development of model 4 is presented in Figure 9 and shows the nature of the UV delay in more detail. The four spectra plotted in the lower panel represent the disk at $t = 2.22$, 2.75, 3.02, and 5.33 days, respectively, from the bottom to the top of the panel and show how the disk evolves from the cool state to visual maximum. The UV continuum is still very weak when the visual luminosity is a factor of ~ 10 below maximum, and most of the disk has a temperature of ~ 6000–8000 K. The UV and optical continua are roughly equal in strength ~ 1 mag below visual maximum, but the UV

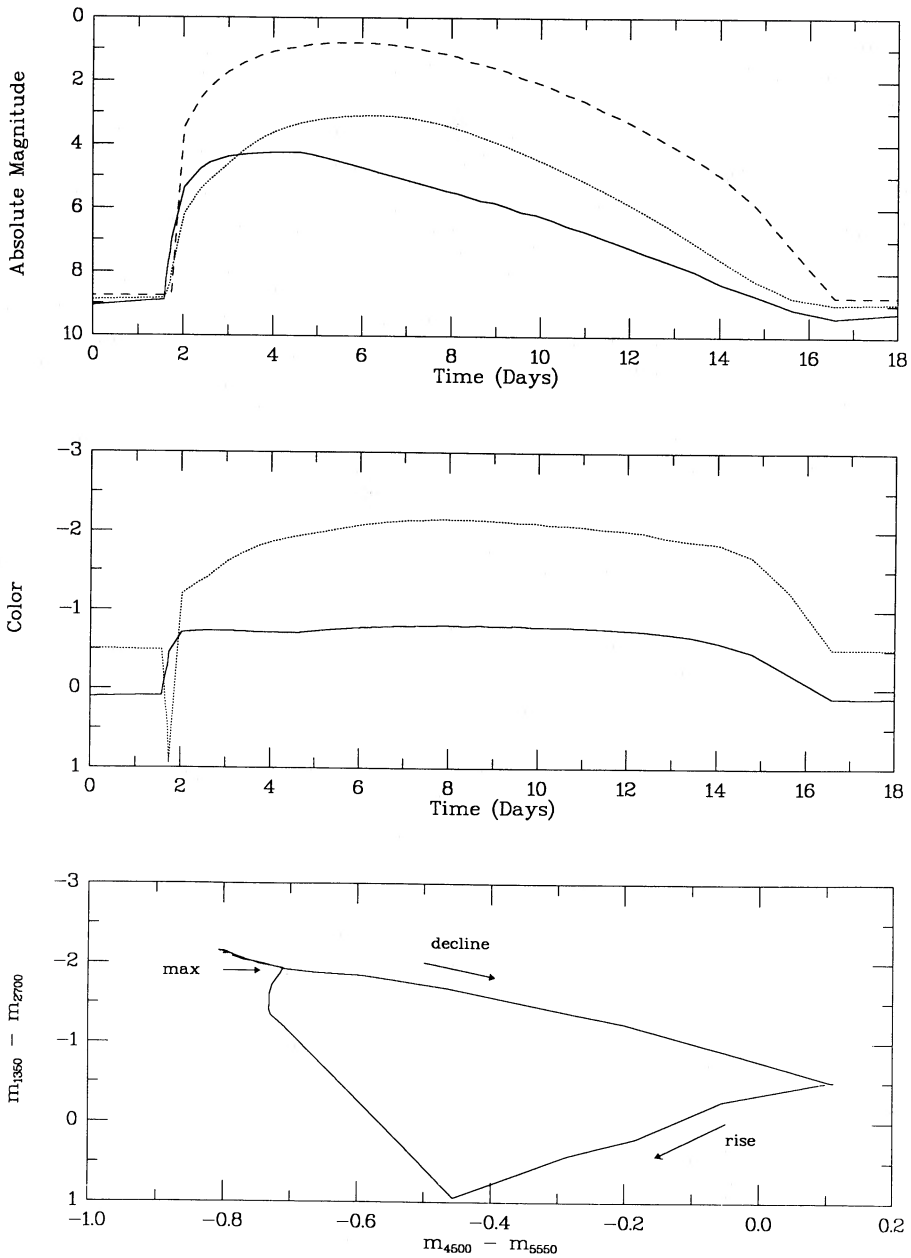

FIG. 8.—Light and color curves for an outside-in eruption in a large disk (Model 4), with panels arranged as in Fig. 2

continues to rise after optical maximum. The C IV absorption line at 1550 Å appears during the late stages of the rise and is very strong when m_{1350} peaks, as shown in the top panel of Figure 9. Prominent C II (log $\lambda = 3.12$) and H I absorption features also appear as the optical flux increases, while Mg II (log $\lambda = 3.45$), Ca II (log $\lambda = 3.6$), and Mg I (log $\lambda = 3.72$) absorption lines fade on the rise to visual maximum.

The decline from UV maximum is shown in the top panel of Figure 9; spectra at $t = 6.66$, 13.86, 16.62, and 17.58 days are plotted from top to bottom in this panel. The H I absorption lines noticeably weaken during the decline of the optical flux; the Na I D lines appear weakly at visual maximum and strengthen considerably as V increases. The strong UV lines weaken as well: C IV disappears between $t = 13$ days and $t = 15$ days, and lines near 1300 Å vanish shortly thereafter. Although it is very difficult to extract absorption-line equivalent widths in dwarf novae (they are blended with emission lines), the appearance and disappearance of various absorption features might provide an independent measure of the disk temperature throughout the course of an eruption.

As with models 1 and 2, steady-state disks provide a poor representation of the spectrum during the decline of the time-dependent disks in models 3 and 4. The temperature gradients in the larger disks are more similar to the $d \log T/d \log R = -0.75$ expected in a steady disk than those of models 1 and 2, but the deviations from the steady-state prediction are large ($\sim$0.1–0.2 in $d \log T/d \log R$) in the inner and outer portions of the disk. These results suggest that time-dependent disks are 0.5–1.0 mag brighter than steady-state disks when the $m_{1350} - m_{2700}$ colors are identical. This conclusion should be

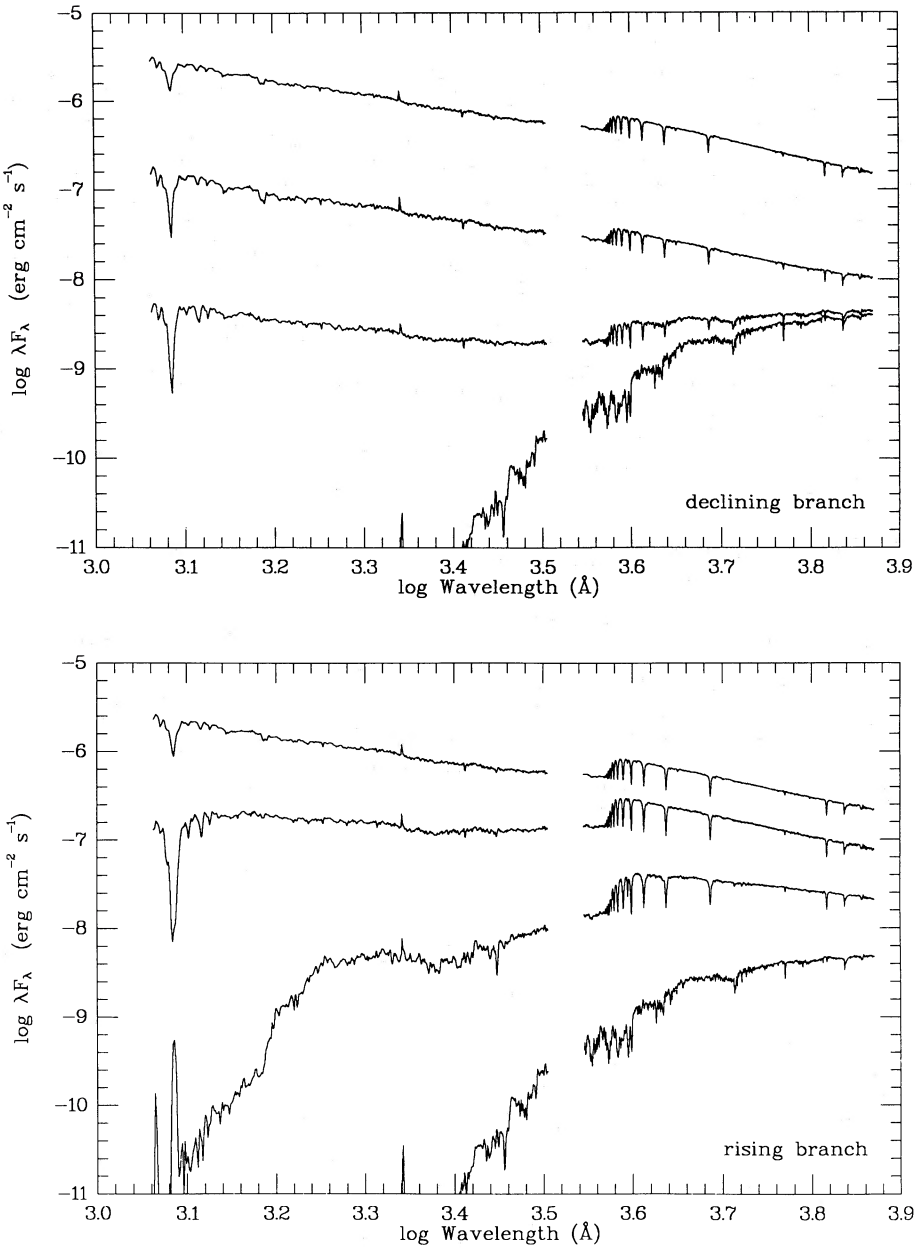

FIG. 9.—Evolution of the disk spectrum during an outside-in eruption (Model 4), with panels arranged as in Fig. 3. The lower panel plots spectra for $t = 0.27$, 2.75, 3.02, and 5.33 days, while spectra at $t = 6.66$, 13.86, 16.62, and 17.58 days are shown in the upper panel.

accepted with some caution, as it is based on analysis of eruptions in only two accretion disks.

We also caution against overinterpretation of the behavior of absorption features in our models. The evolution of absorption-line equivalent widths in dwarf nova eruptions is a complicated function of the vertical disk structure in each annulus, and it cannot be expected that absorption lines in a disk will resemble those observed in the main-sequence stars used in our calculations. The appearance and disappearance of certain ions (such as Mg II, for example) will depend mainly on the photospheric temperature of the disk, and thus we have stressed the presence or absence of certain lines rather than line strengths or line profiles.

IV. DISCUSSION

The results described in the previous section are in good agreement with those of other investigators for inside-out dwarf nova outbursts, in which the eruption begins near the inner edge of the disk (cf. Smak 1984*b*; CWP; PVW). We find that the optical and ultraviolet flux rise nearly simultaneously and estimate that the optical leads the UV by less than ~ 0.01 day. Aside from differences in the absolute magnitude at maximum, the spectral evolution of a given inside-out burst appears to be independent of the size of the disk. The light and color curves will, of course, depend on the α's and $R_{\rm inj}$, but otherwise the physical behavior of inside-out bursts should be similar from one CV to the next.

Outside-in bursts are much more interesting than inside-out bursts, as their behavior does depend on the size of the accretion disk. Our results suggest that *the UV flux lags the optical flux for all outside-in eruptions regardless of the size of the accretion disk.* However, the length of the delay is quite sensitive to the outer disk radius: we found a delay of ~ 0.1 day for a small disk and ~ 0.25 day for a larger disk. These delays are similar to those derived by PVW but shorter than those deduced from a consideration of blackbody disk models.

Eruptions in which the optical flux leads the far-UV flux by $\Delta t \lesssim 1$ day have now been observed in both long and short orbital period dwarf novae: e.g., VW Hyi ($P = 1.8$ hr; $\Delta t \sim 0.5$–1.0 day; Schwarzenberg-Czerny *et al.* 1985; Hassall *et al.* 1983) and SS Cyg ($P = 6.6$ hr; $\Delta t \sim 0.5$–0.75 day; Polidan and Holberg 1984; CWP). The "asymmetric" light curves observed in these systems are consistent with the form expected for outside-in disk instabilities, but, as discovered by PVW and confirmed in this study, the theoretical delay between the rise of the optical and far-UV fluxes is much smaller than observed for short-period systems when standard assumptions are employed. If our knowledge of accretion disk physics were complete, this disagreement would be a serious blow to the disk instability theory for dwarf nova eruptions. However, there are several physically realistic modifications to the standard theory which deserve serious consideration.

1. In our models, material is added to the disk at $R_{\rm inj} \sim 0.5R_{\rm out}$, so eruptions necessarily begin at $R < R_{\rm inj} \ll R_{\rm out}$. If we assume that the delay in the rise of the UV continuum is roughly proportional to the radius at which disk material first evolves to the high state, then the maximum UV delay would be achieved for a burst beginning at $R = R_{\rm out}$. This maximum delay is $\Delta t \sim 0.4$ day for a 1 hr CV and $\Delta t \sim 0.75$ day for a 6 hr CV system and might be achieved if incoming material having an angular momentum per unit mass of $v_{\rm inj} R_{\rm inj}$ mixes with material in the outer disk, such that its equilibrium radius is intermediate between $R_{\rm inj}$ and $R_{\rm out}$ (Bath and Pringle 1982). In some sense, the "zero viscosity radius" $R_{\rm inj}$ represents a lower limit to the point at which matter arriving from the secondary can come to rest (Lubow and Shu 1975; Sulkanen, Brasure, and Patterson 1981). A more physical alternative might be to add material at the outer disk radius and require $R_{\rm out}$ to be equal to the disk's tidal radius ($\approx 0.8R_{\rm RL,wd}$, where $R_{\rm RL,wd}$ is the radius of the white dwarf's Roche lobe). Although Δt may be increased by modifications to *our* calculations, PVW still found very small UV delays for disk instability models using Bath and Pringle's (1982) method of adding material to the disk.

2. Theoretical investigations of the disk instability mechanism have thus far employed scaling laws for the viscosity in which the lower stable branch terminates at $T \sim 6000$ K. If the loci of equilibrium solutions actually lie at temperatures of ~ 2000–3000 K (CGW; CW), then the disk would require a longer time to generate hot material during the onset of an outburst. This prescription would delay the rise of the far-UV flux relative to the optical and has been suggested as an explanation for observations of VW Hyi (Hassall 1984) by Meyer-Hofmeister (1987).

3. It is unfortunate that the magnitude of the UV delay depends on the "recipe" used to calculate the flux distribution. Large delays (~ 1 day) have been found for "blackbody" disks (Smak 1984*b*; CWP), while smaller delays ($\lesssim 0.5$ day) characterize "stellar" disks (PVW; this paper). The source of this difference involves the large opacity shortward of the hydrogen Lyman and Balmer limits in stars with effective temperatures of $\sim 10{,}000$ K, which raises the flux distribution longward of ~ 1200 Å and 4000 Å over that of a blackbody at the same temperature. The fact that the Balmer absorption jump observed in erupting dwarf novae is much smaller than predicted by standard stellar atmosphere techniques (Hassall 1985; Wade 1984; PVW) is an important piece of evidence suggesting that the true radiative transfer solution lies somewhere between the two extremes modeled to date. Calculations described by Shaviv and Wehrse (1986) are a small step in the right direction; more rigorous radiative transfer computations are needed to determine the importance of the Lyman and Balmer limits on the UV delay.

It remains to be seen if such "improvements" in the theory will be sufficient to increase the delay to the observed value of ~ 1 day in short-period CVs.

The merits and deficiencies of dwarf nova eruption mechanisms have been debated ad nauseum (cf. Smak 1984*a*; Bath 1985; PVW; and references therein), but it is difficult to choose between two theories with an apparently inexhaustible supply of free parameters. Progress has been made with simultaneous optical/ultraviolet observations of several CVs (e.g., Hassall *et al.* 1983; Verbunt *et al.* 1984; CWP; PVW), but comprehensive coverage of dwarf novae with symmetric and asymmetric optical light curves is needed to derive useful constraints on the theories over a range of orbital periods and other physical parameters. Such observations are not easy to obtain with *IUE*, so it is important to identify other diagnostics which can test the theories.

One probe of the dwarf nova eruption mechanism could be the "dwarf nova oscillations" (DNOs), *coherent oscillations with periods ~ 10–40 s that appear near visual maxima* (cf. Warner 1976; Robinson and Nather 1979; Patterson 1981). The periods of DNOs *decrease* during the rise to visual maxima, and typically reach a minimum period ~ 1–2 days *following* visual maximum (i.e., near UV maximum). The DNO period increases slowly during the decline of a dwarf nova, and the oscillations disappear before the system returns to quiescence. Patterson (1981, and references therein) noted that the relationship between DNO period and visual intensity is $d \log P/d \log I \approx 0.2$ for a variety of CVs, including Z Cam, SY Cnc, AH Her, and KT Per.

The fact that the period of a DNO reaches a minimum when the UV continuum is at a maximum suggests that the DNOs may be a useful probe of the accretion rate onto the white dwarf. The most promising physical mechanism for producing DNOs involves nonradial pulsations of a rotating, accreting white dwarf (Papaloizou and Pringle 1978), and it seems plausible that the decrease in period of DNOs during a rise to visual maximum is caused by an increase in the accretion rate into the outer atmosphere of the central white dwarf. If our connection of DNOs with an increased flow of mass through the disk is correct, then high-speed photometry of dwarf nova eruptions would be capable of monitoring the behavior of the inner disk and the outer disk simultaneously.

An examination of DNOs described by Patterson (1981) lends some support for our proposal. Dwarf novae with asymmetric optical light curves tend to have asymmetric "period curves" as well, in that the rate of change of DNO periods closely follows the optical light curve. CVs with symmetric visual light curves (such as GK Per; Cannizzo and Kenyon 1986) are not well represented in Patterson's list, but the evolution of V and DNO period in RU Peg are fairly symmetric in

time. The evolution of the DNO suggests RU Peg may experience "inside-out" eruptions, and it is important to identify DNOs in other CVs with symmetric optical light curves.

V. SUMMARY

We have described the spectral evolution of disk instability models for dwarf nova eruptions. Our major results can be summarized as follows.

1. Eruptions in disks with low background accretion rates begin near the white dwarf and quickly spread to larger disk radii. The continuum flux rises simultaneously at all wavelengths in these "inside-out" outbursts, and light curves at 1350 Å and at V have round, symmetric maxima.

2. Outbursts in disks with higher mass-transfer rates commence near the outer edge of the disk. The optical continuum flux rises before the UV continuum by $\sim$0.1–0.3 day for the parameters chosen in this study, which is smaller than the $\sim$0.5–1.0 day delays observed in several dwarf novae. Some of the "standard assumptions" used in disk instability models must be modified to bring the theory into accord with the observations. We have suggested that changing the method of adding material to the disk or modifying the treatment of radiative transfer in the disk might increase the theoretical delay in the rise of the UV continuum to $\sim$1 day.

3. Dwarf nova oscillations (DNOs) could be an important probe of the dwarf nova eruption mechanism. It appears that the minimum period in DNOs coincides with the peak in the UV continuum flux, which suggests that the period variations observed in most dwarf novae might be used to determine the source of the eruptions.

The authors would like to acknowledge useful conversions with G. Berriman, J. Gallagher, L. Hartmann, C. Mauche, F. Meyer, E. Meyer-Hofmeister, R. Polidan, J. Raymond, A. Shafter, F. Verbunt, B. Warner, R. Webbink, and J. C. Wheeler. We give special thanks to R. Wade for comments during the course of this study, and for an excellent referee's report which improved the presentation of our results. This work was supported in part by the National Aeronautics and Space Administration through grant NGR 22-007-272 to the Harvard-Smithsonian Center for Astrophysics and by NSERC grant 5-37687 at McMaster University (J. K. C.).

REFERENCES

Barnes, T. G., Evans, D. S., and Moffett, T. J. 1978, *M.N.R.A.S.*, **183**, 285.
Bath, G. T. 1985, *Rept. Prog. Phys.*, **48**, 483.
Bath, G. T., and Pringle, J. E. 1981, *M.N.R.A.S.*, **194**, 967.
———. 1982, *M.N.R.A.S.*, **199**, 267.
Berriman, G. 1984, *M.N.R.A.S.*, **210**, 223.
Berriman, G., Kenyon, S., and Bailey, J. 1986, *M.N.R.A.S.*, **222**, 871.
Berriman, G., Kenyon, S., and Boyle, C. 1987, *A.J.*, submitted.
Cabot, W., Canuto, V. M., Hubickyj, O., and Pollack, J. B. 1986, preprint.
Cannizzo, J. K., Ghosh, P., and Wheeler, J. C. 1982, *Ap. J. (Letters)*, **260**, L83 (CGW).
Cannizzo, J. K., and Kenyon, S. J. 1985, in *Proc. 9th North American Workshop on Cataclysmic Variables*, ed. P. Szkody (Seattle: University of Washington), p. 6.
Cannizzo, J. K., and Kenyon, S. J. 1986, *Ap. J. (Letters)*, **309**, L43.
Cannizzo, J. K., Shafter, A. W., and Wheeler, J. C. 1987, *Ap. J.*, submitted.
Cannizzo, J. K., and Wheeler, J. C. 1984, *Ap. J. Suppl.*, **55**, 367 (CW).
Cannizzo, J. K., Wheeler, J. C., and Polidan, R. S. 1986, *Ap. J.*, **301**, 634 (CWP).
Code, A. D., Davis, J., Bless, R. C., and Hanbury Brown, R. 1986, *Ap. J.*, **203**, 417.
Córdova, F. A., and Mason, K. O. 1982, *Ap. J.*, **260**, 716.
Faulkner, J., Lin, D. N. C., and Papaloizou, J. 1983, *M.N.R.A.S.*, **205**, 359 (FLP).
Ferguson, D. H. 1983, Ph.D. thesis, University of Arizona.
Hassall, B. J. M. 1984, in *Proc. Fourth European IUE Conference*, ed. E. Rolfe and B. Battrick (Rome: ESA SP-218), p. 385.
Hassall, B. J. M. 1985, *M.N.R.A.S.*, **216**, 335.
Hassall, B. J. M., Pringle, J. E., Schwarzenberg-Czerny, A., Wade, R. A., Whelan, J. A. J., and Hill, P. W. 1983, *M.N.R.A.S.*, **203**, 865.
Hassall, B. J. M., Pringle, J. E., and Verbunt, F. 1985, *M.N.R.A.S.*, **216**, 353.
Herter, T., Lacasse, M. G., Wesemael, F., and Winget, D. E. 1979, *Ap. J. Suppl.*, **39**, 513.
Hoshi, R. 1979, *Prog. Theor. Phys.*, **61**, 1307.
Jacoby, G. H., Hunter, D. A., and Christian, C. A. 1984, *Ap. J. Suppl.*, **56**, 257.
Johnson, H. L. 1966, *Ann. Rev. Astr. Ap.*, **4**, 193.
Kenyon, S. J., and Webbink, R. F. 1984, *Ap. J.*, **279**, 252.
Klare, G., *et al.* 1982, *Astr. Ap.*, **113**, 76.
Krautter, J., *et al.* 1981, *Astr. Ap.*, **102**, 337.
la Dous, C., *et al.* 1985, *M.N.R.A.S.*, **212**, 231.
Lin, D. N. C., Papaloizou, J., and Faulkner, J. 1985, *M.N.R.A.S.*, **212**, 105 (LPF).
Lubow, S. H., and Shu, F. H. 1975, *Ap. J.*, **198**, 383.
Lynden-Bell, D., and Pringle, J. E. 1974, *M.N.R.A.S.*, **168**, 603.
Mayo, S. K., Wickramasinghe, D. T., and Whelan, J. A. J. 1980, *M.N.R.A.S.*, **193**, 793.
Meyer, F. 1984, *Astr. Ap.*, **131**, 303.
Meyer, F., and Meyer-Hofmeister, E. 1981, *Astr. Ap.*, **104**, L10 (MM81).
Meyer, F., and Meyer-Hofmeister, E. 1982, *Astr. Ap.*, **106**, 34 (MM82).
———. 1984, *Astr. Ap.*, **132**, 143 (MM84).
Meyer-Hofmeister, E. 1987, in *IAU Colloquium 93, Cataclysmic Variables*, ed. H. Drechsel, J. Rahe, and Y. Kondo (Dordrecht: Reidel), in press.
Mineshige, S., and Osaki, Y. 1983, *Pub. Astr. Soc. Japan*, **35**, 377 (MO83).
———. 1985, *Pub. Astr. Soc. Japan*, **37**, 1 (MO85).
Osaki, Y. 1974, *Pub. Astr. Soc. Japan*, **26**, 429.
Papaloizou, J. Faulkner, J., and Lin, D. N. C. 1983, *M.N.R.A.S.*, **205**, 487 (PFL).
Papaloizou, J., and Pringle, J. E. 1978, *M.N.R.A.S.*, **182**, 423.
Patterson, J. 1981, *Ap. J. Suppl.*, **45**, 517.
Polidan, R. S., and Holberg, J. B. 1984, *Nature*, **309**, 528.
Pringle, J. E., Verbunt, F., and Wade, R. A. 1986, *M.N.R.A.S.*, **221**, 169 (PVW).
Robinson, E. L., and Nather, R. E. 1979, *Ap. J. Suppl.*, **39**, 461.
Schwarzenberg-Czerny, A., and Różyczka, M. 1977, *Acta Astr.*, **27**, 429.
Schwarzenberg-Czerny, A. *et al.* 1985, *M.N.R.A.S.*, **212**, 645.
Shafter, A. W., Szkody, P., Liebert, J., Penning, W. R., Bond, H. E., and Grauer, A. 1985, *Ap. J.*, **290**, 707.
Shafter, A. W., Wheeler, J. C., and Cannizzo, J. K. 1986, *Ap. J.*, **305**, 261 (SWC).
Shakura, N. I., and Sunyaev, R. A. 1973, *Astr. Ap.*, **24**, 337.
Shaviv, G., and Wehrse, R. 1986, *Astr. Ap.*, **159**, L5.
Smak, J. 1982, *Acta Astr.*, **32**, 199.
———. 1984*a*, *Pub. A.S.P.*, **96**, 5.
———. 1984*b*, *Acta Astr.*, **34**, 161.
Sulkanen, M. E., Brasure, L. W., and Patterson, J. 1981, *Ap. J.*, **244**, 579.
Szkody, P. 1981, *Ap. J.*, **247**, 577.
———. 1982, *Ap. J.*, **261**, 200.
———. 1985, *A.J.*, **90**, 1837.
Szkody, P., and Mateo, M. 1984, *Ap. J.*, **280**, 729.
Tylenda, R. 1977, *Acta Astr.*, **27**, 235.
———. 1981, *Acta Astr.*, **31**, 127.
Verbunt, F., *et al.* 1984, *M.N.R.A.S.*, **210**, 197.
Wade, R. A. 1982, *A.J.*, **87**, 1558.
———. 1984, *M.N.R.A.S.*, **208**, 381.
Warner, B. 1976, in *IAU Symposium 73, The Structure and Evolution of Close Binary Systems*, ed. P. Eggleton, S. Mitton, and J. Whelan (Dordrecht: Reidel), p. 85.
Whyte, C. A., and Eggleton, P. P. 1980, *M.N.R.A.S.*, **190**, 801.
Williams, R. E. 1980, *Ap. J.*, **235**, 939.
Wood, J., Horne, K., Berriman, G., Wade, R., O'Donoghue, D., and Warner, B. 1986, *M.N.R.A.S.*, **219**, 629.
Wu, C.-C., *et al.* 1983, *The Ultraviolet Spectral Atlas, IUE NASA Newsletter*, No. 22.
Wu, C.-C., and Panek, R. J. 1982, *Ap. J.*, **262**, 244.
———. 1983, *Ap. J.*, **271**, 754.

J. K. CANNIZZO: Department of Physics, McMaster University, Hamilton, ON L8S 4M1, Canada

S. J. KENYON: Smithsonian Astrophysical Observatory, 60 Garden Street, Cambridge, MA 02138